# 6

# Combustion and Flame

The main function of the rotary kiln in the minerals and materials industry is to convert raw materials (ore) into useful product materials. The kiln also has become the workhorse in waste destruction and remediation in the environmental industry. Most or all of these processes involve some chemical or physical reactions that will occur at economically rapid rates, if at all, only at high temperatures. We must therefore get energy into the process as well as later extract it. In materials processing, it is often impractical to supply energy mechanically, that is, by work, which means that heat transfer is usually the way to drive these operations. We will treat kiln heat transfer in the chapters that follow but for now we will examine the energy source and supply of the required heat. Although a handful of small-size indirectly heated kilns might use electrical energy to process material, for most large processing operations the dominant source of energy is fossil fuel combustion. Therefore the flame that develops from fuel firing is the heart of the direct-fired rotary kiln.

## 6.1 Combustion

Combustion is the conversion of fossil fuel into chemical compounds (or products) by combining it with an oxidizer, usually oxygen in air. The combustion process is an exothermic chemical reaction, that is, a reaction that releases heat energy as it occurs.

$$\text{Fuel} + \text{Oxidizer} \rightarrow \text{Products of combustion} + \text{Energy} \qquad (6.1)$$

Here the fuel and the oxidizer are the reactants, that is, the substances that were present before the reaction took place. The relation indicates that the reactants produce combustion products and energy but as it is known in the "fire triangle", there must also be an ignition source for it to proceed. The amount of heat released during combustion depends upon the type of fuel. Fuels are evaluated based on the amount of energy or heat they release per unit mass, per volume, or per mole during combustion of the fuel. This quantity is known as the fuel's heat of reaction or its heating value and is usually expressed in specific terms such as J/kg (Btu/lb), kcal/liter (Btu/gal), kcal/$m^3$ (Btu/$ft^3$), and so on. Physically, the heat released may be characterized by the intensity of the flame and also by its luminosity. The effectiveness of dissipating this heat may be judged by the flame shape. Since the kiln operator has no control over the heat content of the fuel (usually dependent on its source), the success of all kiln operations lies in the effectiveness of controlling the flame to ensure that the temperature profile in the freeboard matches the intended material process. In most combustion systems and for that matter in rotary combustion chambers, the oxidizer is usually air but it could be either pure oxygen or an oxygen mixture. For practical reasons we will limit our attention to combustion of fuel with oxygen or air as the main source of the oxidant. Chemical fuels exist in various forms including gaseous, liquid, and solid forms. Common fuels that are burnt in most kilns are either solids (e.g., coal or coke), liquids (e.g., residual oils), or gases (e.g., natural gas, coke oven gas). Some kiln operations are permitted to burn liquid hazardous wastes. In the United States these may require either an incinerator's permit or the Boiler and Industrial Furnace (BIF) permit that allows use of some waste fuels to supplement fossil fuels to produce useful industrial product. Waste fuels include all types of solids such as used tires, contaminated grease rags, and liquid solvents such as alcohols, esters, and so on, that may collectively be called liquid burnable materials (LBM). Although some of these waste fuels have energy contents that are comparable to coal or diesel oil, solvents are usually lighter liquid fuels that can result in low luminosity flame upon combustion. Some of the negative attributes of LBM are high moisture content, low carbon content, and high concentration of noncombustible impurities.

In the case of gaseous fuels it is common practice to analyze the mixture for the component gases and to report the analysis in terms of volume (or mole) percent. This is essential because most gaseous fuels are mixtures of only a few chemical compounds. On the other

hand, naturally occurring or commercially available organic liquids or solids (including coal) can contain thousands of compounds, many of which have very complex molecular structure. These are usually analyzed for the weight percentages of the elements of carbon, hydrogen, nitrogen, oxygen, and sulfur that are present in the fuel, that is, C:H:N:O:S. In kiln process design and operation it is common practice to establish mass and mole fractions of the intended fuel so as to design the appropriate burners for the kiln process and to keep track of emissions during kiln operations.

## 6.2 Mole and Mass Fractions

The amount of a substance in a fuel sample may be indicated by its mass or by the number of moles of that substance. A mole is defined as the mass of a substance equal to its molecular mass or molecular weight. Gram-mole or pound mole of C:H:N:O:S is 12:2:28:32:32 kg or $lb_m$. The mass fraction of a component $i$, $mf_i$ is defined as the ratio of the mass of the component, $m_i$, to the mass of the mixture, $m$, that is,

$$mf_i = \frac{m_i}{m} \tag{6.2}$$

where the sum of the mass fractions of all components must equal 1, as

$$mf_1 + mf_2 + mf_3 + \cdots = 1 \tag{6.3}$$

An analogous definition for the mole fraction of a component, $i$, $x_i$, is the ratio of the number of moles of $i$, $n_i$, to the total number of moles in the mixture, $n$, that is,

$$x_i = \frac{n_i}{n} \tag{6.4}$$

where $n = n_1 + n_2 + \cdots$ and $n_1 + n_2 + n_3 + \cdots = 1$

Thus the mass of a component $i$ of a mixture is the product of the number of moles of $i$ and the molecular weight, $M_i$, that is, the total mass is therefore the sum

$$m = n_1 M_1 + n_2 M_2 + \cdots$$

Dividing and multiplying the right-hand side by the total number of moles, $n$, and invoking Equation (6.4) defines the average molecular weight, that is,

$$M = \frac{m}{n} = x_1 M_1 + x_2 M_2 + \cdots \tag{6.5}$$

The mass fraction of component $i$ is defined as follows

$$mf_i = \frac{n_i M_i}{n_1 M_1 + n_2 M_2 + \cdots} \quad \text{or} \quad mf_i = \frac{x_i M_i}{x_1 M_1 + x_2 M_2 + \cdots} \tag{6.6}$$

For a mixture at a given temperature and pressure, the ideal gas law shows that $pV_i = n_i \Re T$ for any component, and $pV = n\Re T$ for the mixture as a whole. The ratio of these two equations gives

$$x_i = \frac{V_i}{V} = \frac{n_i}{n} \tag{6.7}$$

Similarly, for a given volume of mixture of gases at a given temperature $p_i V = n_i \Re T$ for each component and $pV = n\Re T$ for the mixture. The ratio of these two equations shows that the partial pressure of any component $i$ is the product of the mole fraction and the pressure of the mixture, that is,

$$p_i = \frac{p n_i}{n} = p x_i \tag{6.8}$$

Air, usually used as the oxidant in combustion, contains approximately 21 percent oxygen, 78 percent nitrogen, and 1 percent other inert constituents by volume. Assuming 21 percent $O_2$ and 79 percent $N_2$ by volume for ease of combustion calculations, we have 21 moles of $O_2$ and 79 moles of $N_2$ present in combustion air. Hence $79/21 = 3.76$ moles of nitrogen accompany every mole of oxygen that reacts with the fuel in combustion. At very high temperatures some of the nitrogen will react to form $NO_x$ but at moderate temperatures where the nitrogen is treated as inert, the 3.76 moles of the accompanying nitrogen will end up in the combustion products. Based on the foregoing definitions and equations, the molecular weight of air can be estimated based on the molar fractions on $O_2$ and $N_2$ as follows

$$M_{\text{air}} = \sum n_i M_i = 0.79 M_{N_2} + 0.21 M_{O_2} = 0.79(28) + 0.21(32) = 28.84 \tag{6.9}$$

The mass fractions of oxygen and nitrogen are

$$mf_{O_2} = \frac{n_{O_2} M_{O_2}}{M_{air}} = \frac{(0.21)(32)}{28.84} = 0.233;$$
$$mf_{N_2} = \frac{n_{N_2} M_{N_2}}{M_{air}} = \frac{(0.79)(28)}{28.84} = 0.767 \quad (6.10)$$

## 6.3 Combustion Chemistry

Following Equation (6.1), combustion will be a chemical reaction between fossil fuel atoms (predominantly carbon and hydrogen, i.e., hydrocarbon) and oxygen in air to form carbon dioxide and water vapor. Methane, $CH_4$, is the major constituent of most natural gases and undergoes combustion reaction

$$CH_4 + 2O_2 = CO_2 + H_2O\Delta H(192\,\text{kcal/mol}) \quad (6.11)$$

For coal with C:H:N:O:S as constituents, the individual combustible fuel fraction molecules will undergo combustion described by the following reactions

$$C + 2O_2 = CO_2 + \Delta H(393.7\,\text{kJ/mol}) \quad (6.12)$$
$$2H_2 + O_2 = 2H_2O + \Delta H(285\,\text{kJ/mol}) \quad (6.13)$$
$$C + O_2 = 2CO + \Delta H(110.6\,\text{kJ/mol}) \quad (6.14)$$
$$S + O_2 = SO_2 + \Delta H(297\,\text{kJ/mol}) \quad (6.15)$$

Suffice it to say that carbon dioxide is the product formed by complete combustion. Incomplete combustion will yield CO, a toxic compound, which can further be oxidized to $CO_2$. The toxicity of CO comes from the fact that when inhaled it forms oxy-hemoglobin in the bloodstream which prevents hemoglobin from absorbing oxygen.

The coefficients in the chemical reactions of combustion may be interpreted as the number of moles of the substances required for the reactions to occur. For example, in the methane combustion reaction, 1 mole of methane reacts with 2 moles of oxygen to form 1 mole of carbon dioxide and 2 moles of water. Although the number of atoms of each element must be conserved during a reaction, the total number of moles or molecules need not. Because the number of atoms of each element cannot change, it follows that the mass of each element and

the total mass must be conserved. Hence, using the atomic weights or the masses of each element, the sums of the masses of the reactants and the products must be balanced.

$$\mathrm{CH_4} + 2\mathrm{O_2} = \mathrm{CO_2} + 2\mathrm{H_2O}$$
$$[12 + 4(1)] + 2(32) = [12 + 2(16)] + 2[2(1) + 16] = 80 \qquad (6.16)$$

Additionally, there are 2 moles of water and 1 mole of $CO_2$ in the 3 moles of combustion products. Therefore the mole fraction of water and carbon dioxide in the combustion products are

$$x_{\mathrm{H_2O}} = 0.667; \quad x_{\mathrm{CO_2}} = 0.333 \qquad (6.17)$$

But there are 2(18) mass units of water and 44 mass units of $CO_2$ in the 80 mass units in the products, so the mass fractions are 36/80 and 44/80 respectively, that is,

$$mf_{\mathrm{H_2O}} = 0.45; \quad mf_{\mathrm{CO_2}} = 0.55 \qquad (6.18)$$

Analogous fractions can be expressed for the other substances by balancing their combustion equations. Because we know that in air every mole of oxygen is accompanied by 3.76 moles of nitrogen, the methane reaction in air can be written as:

$$\mathrm{CH_4} + 2\mathrm{O_2} + 2(3.76)\mathrm{N_2} = \mathrm{CO_2} + \mathrm{H_2O} + 2(3.76)\mathrm{N_2} \qquad (6.19)$$

Hence with air as an oxidizer instead of oxygen, there are 2 moles of water per 10.52 moles of product, compared with 2 moles of water per 3 moles of products.

Because the combustion products exit the atmosphere through the stack, they are known as the stack gases or flue gases. Oftentimes the flue gas composition is stated on a wet basis (wfg) or on a dry basis (dfg) because under certain conditions the water vapor in the flue gas may condense and escape as liquid water. When the water vapor condenses, the mass of the dry combustion product is used in estimating the mass or mole fraction. The term higher heating value (HHV) of the fuel, frequently used in the United States, refers to a heating value measurement in which the product water condenses. As a consequence the latent heat of vaporization of the water is released and becomes part of the heating value. The lower heating value (LHV), frequently used

in Europe, corresponds to the heating value in which water remains as vapor and does not yield its latent heat of vaporization, that is,

$$\text{HHV} = \text{LHV} + \left(\frac{m_{\text{H}_2\text{O}}}{m_{\text{fuel}}}\right) h_{\text{fg}} \quad [\text{kJ/kg}] \tag{6.20}$$

where $h_{\text{fg}}$ is the latent heat of vaporization of water.

## 6.4 Practical Stoichiometry

When designing a burner for rotary kiln combustion, or for any combustion chamber for that matter, it is important to establish the amount of air required for the combustion reaction. This requirement includes sizing the burner nozzle to an air velocity that will induce all the jet properties appropriate to the operation, and ensure optimum energy savings with minimum environmental pollutants. The aim of practical stoichiometry is to determine exactly how much air must be used to completely oxidize the fuel to the combustion products. A stoichiometrically correct mixture of fuel and air is defined as one that would yield exactly the products and have no excess oxygen if combustion were complete. Knowing the stoichiometric amount, the burner designer can decide how much excess air would be needed to ensure the appropriate jet character and flame temperature, among others. In general, one can write a balanced stoichiometric relationship for any CHNOS fuel-air system as follows

$$\begin{aligned} \text{C}_u\text{H}_v\text{O}_w\text{N}_x\text{S}_y + \left(u + \frac{v}{4} - \frac{w}{2} + y\right)(\text{O}_2 + 3.76\text{N}_2) \\ \rightarrow u\text{CO}_2 + \frac{v}{2}\text{H}_2\text{O} + y\text{SO}_2 + \left[3.76\left(u + \frac{v}{2} - \frac{w}{2} + y\right) + \frac{x}{2}\right]\text{N}_2 \end{aligned} \tag{6.21}$$

The negative sign associated with $w$ indicates that less oxygen from air is needed for complete oxidation because atoms of oxygen already exist in the fuel itself. In most situations it is convenient to normalize the actual mixture composition to the stoichiometric mixture composition for that fuel-oxidizer system. The normalization yields a dimensionless number whose magnitude tells us how far the mixture composition has deviated from stoichiometric conditions. The most

convenient dimensionless number used in practical combustion is the equivalence ratio, Φ, defined as:

$$\Phi = \frac{m_{\text{fuel}}/m_{\text{air}}}{(m_{\text{fuel}}/m_{\text{air}})_{\text{stoich}}} \tag{6.22}$$

or, on a molar basis,

$$\Phi = \frac{n_{\text{fuel}}/n_{\text{air}}}{(n_{\text{fuel}}/n_{\text{air}})_{\text{stoich}}} \tag{6.23}$$

With this definition, mixtures with $\Phi < 1$ are said to be fuel-lean while those with $\Phi > 1$ are said to be fuel-rich. Two other dimensionless ratios that are commonly used to specify the composition of a combustible mixture relative to the stoichiometric composition are the percent theoretical air and percent excess air. These are defined respectively as $100/\Phi$ and $100(1/\Phi - 1)$. Thus, a mixture that has $\Phi = 0.8$ can also be said to contain 125 percent theoretical air or 25 percent excess air.

## 6.5 Adiabatic Flame Temperature

The adiabatic flame temperature is one that occurs when the combustion chamber is well insulated with no heat losses (adiabatic conditions). The peak adiabatic flame temperature occurs at around $\Phi = 1$ in an ideally insulated combustion chamber. Figure 6.1 is a typical graph of flame temperature for a natural gas–air mixture. As percent combustion air increases, that is, as we deviate from the stoichiometric condition, some of the heat generated is used to heat up the excess air. As a result, the flame temperature will drop. By the same token, it is important to note that increasing the fuel at stoichiometric conditions will reduce the flame temperature as is indicated by the left-hand side of the temperature peak in Figure 6.1. Therefore, under controlled conditions, flame temperature can be a useful measure of air-fuel ratio, that is, how far we deviate from stoichiometric conditions and whether the combustion is fuel-lean or fuel-rich. Note that although we have illustrated flame temperature with stoichiometric air (100 percent), the same general rules apply to any combustion condition. This is helpful because it allows temperature control by changing the air-fuel mixture. It also gives us a sense of whether unburned fuel is being released into the atmosphere. In order to maintain the flame temperature at any set of conditions, one must increase or decrease

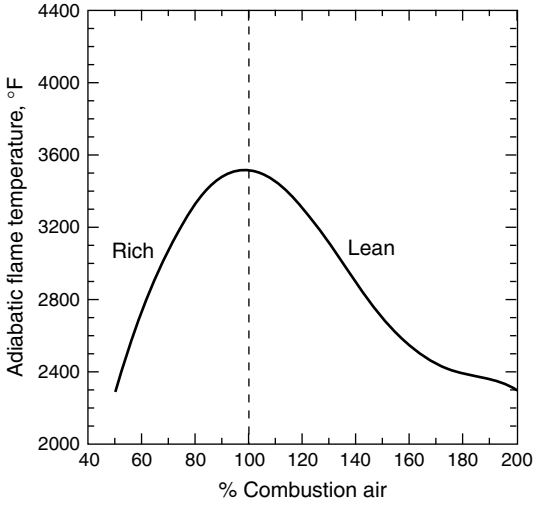


**Figure 6.1** Flame temperature versus air-fuel ratio.

the fuel and air proportionately. Increasing fuel alone or air alone will result in a change in flame temperature. Such a temperature control mechanism is no different from that encountered in the carburetor of spark-ignition automobile engines.

Controlling the air-fuel ratios not only controls the flame temperature but also controls the flame shape or the character of the burning jet. The flame shape can be illustrated by considering the aeration of a simple laminar Bunsen burner jet flame (Figure 6.2). The example shows four systems for introducing air to the fuel in the nozzle. These include nozzle mix, premix, atmospheric, and use of raw fuel without any aeration. Figure 6.2 hypothetically illustrates the expected flame geometry for gaseous fuel as primary aeration diminishes from 100 percent to zero; 100 percent primary air would correspond to a sharp pale blue flame. This is because all of the air for combustion is mixed with the fuel and is ready to ignite as soon as it reaches the nozzle. A flame burning with 75 percent primary air would be characterized by a double blue cone and would be a little longer than the previous one. This is because 25 percent of the fuel molecules will need time to find oxygen from the surrounding air before burning. At 25 percent primary air, only a slight amount of blue color remains in the flame; the flame becomes much longer and predominantly yellow in color. When fuel is burned without any premixing, the flame is normally lazy or ragged; it is very long and all yellow. Assuming that all the fuel

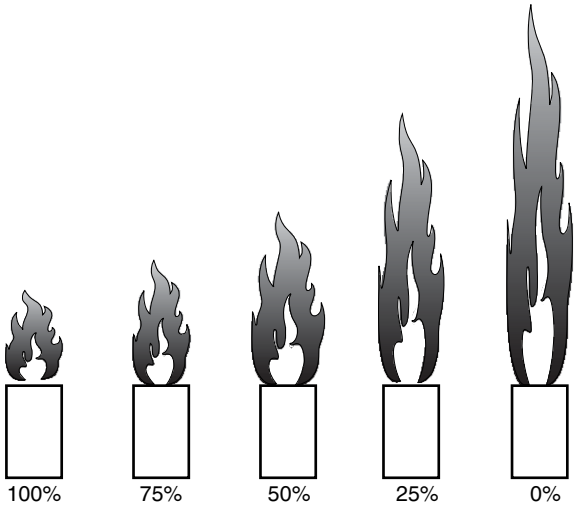


**Figure 6.2** Aeration effect on flame shape.

molecules are burned in each case, then the same amount of energy would be generated.

## 6.6 Types of Fuels Used in Rotary Kilns

Kilns can be fired with natural gas, fuel oil, pulverized solid fuels, or a combination of all of these. As mentioned earlier, the fuel can also include waste fuels. Because of the long gas residence time in the freeboard, kilns have become the combustion chamber of choice for hazardous waste incineration, in some cases achieving 99.99 percent (also referred to as "4-nine") destruction efficiencies. Because most of the rotary kiln operations are high-temperature processes and require intense flames, radiation heat transfer is predominant in the mechanisms of energy transfer to the material being processed. Thermal radiation is also maximized because of the cylindrical enclosure of the freeboard space. Hence fuels having high luminosity as a result of soot formation during combustion tend to improve thermal efficiency and consequently fuel use. Because of the high cost and the transparent nature of natural gas flames, it is normally the last choice of fuel selection for rotary kilns except in places with strict environmental restrictions on $CO_2$ emissions. Most rotary kilns use pulverized fuel, typically coal or petroleum coke as the primary fuel for combustion.

In this section, we will examine the source and types of these fuels and also the factors that maximize their combustion in rotary kilns.

## 6.7 Coal Types, Ranking, and Analysis

Coal consists of a complex range of materials that differ from deposit to deposit. The differences encountered in coal types result from many factors including the vegetation from which the coal originated, the depths of burial of the vegetation from which the coal was formed, the temperatures and pressures at those depths, as well as the length of time the coal has been forming in the deposit. The varying amount of mineral matter in a coal deposit may also have a significant effect on its properties and classification (Table 6.1). The American Society for Testing Materials (ASTM) has established a ranking system that classifies coals as anthracite (I), bituminous (II), sub-bituminous (III), and lignite (IV). Ranking is determined by the degree of transformation of the original plant material to carbon. High-rank coals are high in carbon and therefore heat value, but low in hydrogen and oxygen. Low-rank coals are low in carbon but high in hydrogen and oxygen content. Coal ranking and analysis of combustion rely on two types of analysis of coal composition: the proximate analysis and the ultimate analysis. The proximate analysis involves thermo-gravimetric analysis (TGA) whereby the sample is continuously heated in the absence of oxygen (devolatilization or pyrolysis) in a continuously weighing system. The weight remaining when the temperature of the sample reaches water evaporation temperature determines the moisture content (M). Further weight loss, up to the temperature when no further weight loss occurs, determines the total volatile matter (VM) and the char remaining. The char is composed of carbon and ash so when the remaining sample is burned in air or oxygen until only noncombustible minerals remain (A), the weight loss gives the fixed carbon

**Table 6.1** Proximate Analysis of Some US Coal by Rank (Watson, 1992)

| Source | Rank | M[%] | VM[%] | FC[%] | A[%] | S[%] | BTU/lb |
|---|---|---|---|---|---|---|---|
| Schuylkill, PA | I | 4.5 | 1.7 | 84.1 | 9.7 | 0.77 | 12,745 |
| McDowell, WV | II | 1.0 | 16.6 | 77.3 | 5.1 | 0.74 | 14,715 |
| Sheridan, WY | III | 25.0 | 30.5 | 40.8 | 3.7 | 0.30 | 9,345 |
| Mercer, ND | IV | 37.0 | 26.6 | 32.2 | 4.2 | 0.40 | 7,255 |

(FC). The proximate analysis is usually reported as percentages (or fractions) of the four quantities, that is, moisture, ash, volatile matter, and fixed carbon. The ultimate analysis is a chemical analysis that provides the elemental mass fractions of C, H, N, O, and S usually on a dry, ash-free basis.

$$m = m_{\text{comp}} + m_{\text{ash}} + m_{\text{moist}}$$
$$\frac{m_{\text{comp}}}{m} = 1 - \text{A} - \text{M} \tag{6.24}$$

Thus an equation for the wet and ashy volatile matter fraction in the proximate analysis may be determined from dry, ash-free proximate analysis using the expression

$$\begin{aligned} \text{VM}_{\text{as-fired}} &= \left(\frac{m_{\text{comp}}}{m}\right)(\text{VM})_{\text{dry,ash-free}} \\ &= (1 - \text{A} - \text{M})\,(\text{VM})_{\text{dry,ash-free}} \end{aligned} \tag{6.25}$$

## 6.8 Petroleum Coke Combustion

Petroleum coke (also known as pet coke) is a carbonaceous solid derived from the cracking processes of oil refineries and has been a source of relatively cheap pulverized fuel for the kiln industry. It is called green coke until it is thermally treated into crystalline or calcined pet coke used in the manufacture of electrodes for steel and aluminum extraction. Green coke comes from several sources, all from the petroleum refinery industry. Table 6.2 gives some green coke analyzed by Polak (1971) showing their sources and their elemental analyses.

**Table 6.2** Some Sources of Petroleum Coke and Their Analyses (Polak, 1971)

| Supplier | Site | VM[%] | H[%] | C[%] | S[%] | A[%] | O[%] | N[%] |
|---|---|---|---|---|---|---|---|---|
| Gulf Oil | Canada | 16.2 | 4.18 | 93.4 | 0.73 | 0.08 | — | — |
| Collier | IL | 15.0 | 4.12 | 90.4 | 3.04 | 0.31 | 1.54 | 1.25 |
| Esso | Argentina | 10.6 | 3.66 | 90.7 | 0.76 | 0.49 | 1.21 | 1.67 |
| Standard | OH | 8.8 | 3.73 | 89.6 | 2.86 | 0.12 | 1.83 | 1.32 |
| Humble Oil | LA | 6.6 | 3.69 | 91.8 | 1.50 | 0.16 | — | — |

Heating values range between 14,000–16,000 Btu/lb.

As seen in the table, some pet cokes are good for their low ash content and high carbon content, however their high sulfur content can present environmental problems by emitting $SO_2$, a major source of acid rain, into the atmosphere unless measures are taken to scrub the exhaust gas, which can be very expensive. Hence they are used in the kiln industry by blending it with cheaper, low energy content and high volatile coal to balance emissions and take advantage of their high heating value. Other sources of pulverized fuel include wood and scrap tires, the latter having been used extensively in modern cement kilns.

## 6.9 Scrap Tire Combustion

There are over 280 million scrap tires produced annually in the United States. Of these over 100 million are used as fuel and most of these are burnt to supplement fuel use in cement and other rotary kiln operations. The cement process is particularly convenient for tire combustion because the reinforced steel wire in the tire tread can be a source of iron for the cement chemistry. Kilns burning tires must comply with the EPA's boiler and industrial furnace act and hence are heavily regulated as a pollution source. Table 6.3 gives a typical average composition of tires supplied by the Rubber Manufacturers Association of America.

**Table 6.3** Tire Composition (Rubber Manufacturers Association of America)

| | | Percent Composition | |
|---|---|---|---|
| **Material** | **Chemical Formula** | **Car** | **Truck** |
| Natural rubber | $C_5H_8$ | 12.43 | 24.57 |
| Styrene | $C_8H_8$ | 5.63 | 2.99 |
| 1,3-Butadiene | $C_4H_6$ | 18.34 | 9.75 |
| Fabric | — | 15.47 | 14.85 |
| Carbon Black | C | 24.86 | 25.48 |
| Steel (belt and bead) | — | 18.13 | 17.40 |
| Fillers | — | 5.16 | 4.95 |
| Water (in tires) | $H_2O$ | 0.00 | 0.00 |

Average heating value ≈15,000 Btu/lb.

Combustion of scrap tires and, for that matter, any pulverized fuels including coal, coke, or biomass proceeds in two phases. First, the organic solid polymer undergoes pyrolysis upon reaching a temperature of about 250–300°C to release the volatile matter and solid residue (char). Second, these volatiles and char undergo combustion (Figure 6.3).

Pyrolysis of tires will yield noncondensable gas (mainly CO and $H_2$), pyrolytic oil, and solids (char and metal wire). The proportion of these depends on the pyrolysis temperature, as shown in Figure 6.4.

The char contains carbon black, which is very stable and difficult to burn. A simple analysis based on burning only the volatile component of the pyrolysis (syngas and oil) in a lightweight aggregate kiln (LWA) that typically burns 1 short ton an hour of coal at 26.75 MJ/kg (11,500 Btu/lb) indicates a substantial economic advantage. There is potential savings in replacing 100 percent, 80 percent, and 50 percent (Figure 6.5) of the coal's energy release with tires at two tire pyrolysis temperatures, 950°F (500°C) for the low temperature and 1472°F (800°C) for the high temperature, at a coal price of $37 per ton and a tire price at $20 per ton, delivered. Burning the entire tire including carbon black or finding an alternative use for the carbon black makes tire utilization a lucrative energy-saving proposition.

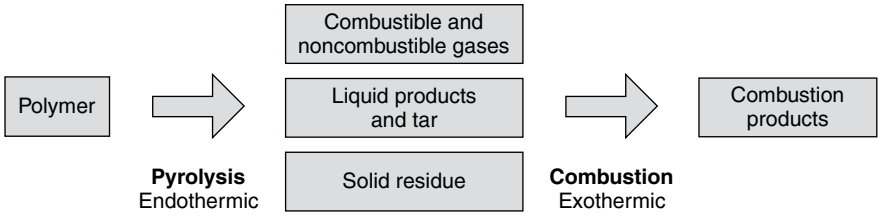


**Figure 6.3** The mechanisms of polymer decomposition and combustion.

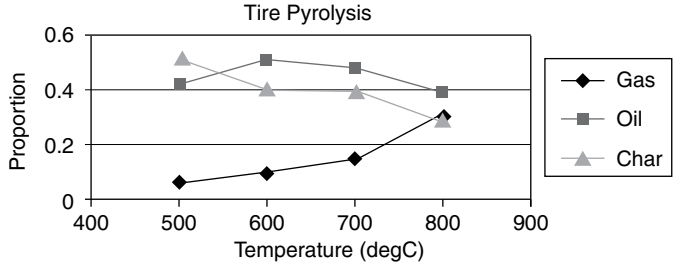


**Figure 6.4** Tire pyrolysis products (UCLLNL-DOE—waste tires).

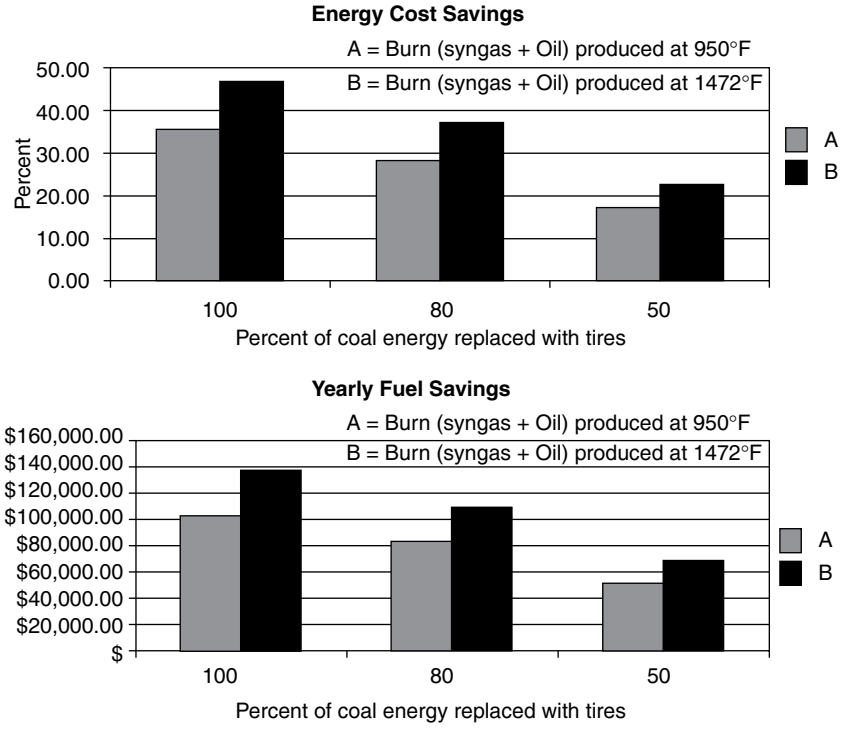


**Figure 6.5** Calculated potential energy and yearly cost savings for scrap tire use in LWA kiln.

## 6.10 Pulverized Fuel (Coal/Coke) Firing in Kilns

Milling of coal or coke produces a powder called pulverized fuel which contains particles of a wide range of sizes. As we saw in Chapter 3, the distance at which a particle in a particle-laden jet will travel in a combustion chamber plays a role in the damping of the jet's turbulent energy. Therefore theoretical analysis of combustion must take the particle size distribution of the fuel into account. Pulverized fuel fineness is therefore an important parameter in the modeling of coal combustion. An analytical expression of particle size distribution that has found a wide application for expressing the fineness of pulverized fuel is the Rosin-Rammler relation. The relationship is given by (Field et al., 1964)

$$R = 100 \exp\left[-(x/x')^n\right] \tag{6.26}$$

where $R$ is the weight percent of particle size greater than $x$, and $x'$ and $n$ are adjustable constants. The constant $x'$ is a measure of the fineness of a powder and is the size, $x$, for which the percent oversize $R$ is $100/e$, that is, 36.8 percent. Although $x'$ is not an average size, it may be related to the weight mean size. The constant $n$ is a measure of size dispersion with a low number indicating a wide size distribution. Equation (6.26) can also be written as

$$\log(\log 100/R) = n \log x + const \tag{6.27}$$

so that a plot of $\log(\log 100/R)$ against $\log x$ should give a straight line with slope $n$. With two known mesh sizes of a particle size analysis, an analytical size distribution of pulverized fuel material can be generated iteratively from Equation (6.26) by first guessing $x'$, calculating components of Equation (6.27), and revising $x'$ until $R$ values match. A distribution where 3 percent weight fraction is retained by 100 US mesh, that is, 150 μm particle size and 77 percent retained by the 200 mesh (75 μm) gives $x' = 108\,\mu m$, $n = 3.82$, and $R = -0.91$ with the distribution shown in Figure 6.6. The parameters can also be estimated using a 2-parameter estimation in a nonlinear regression analysis.

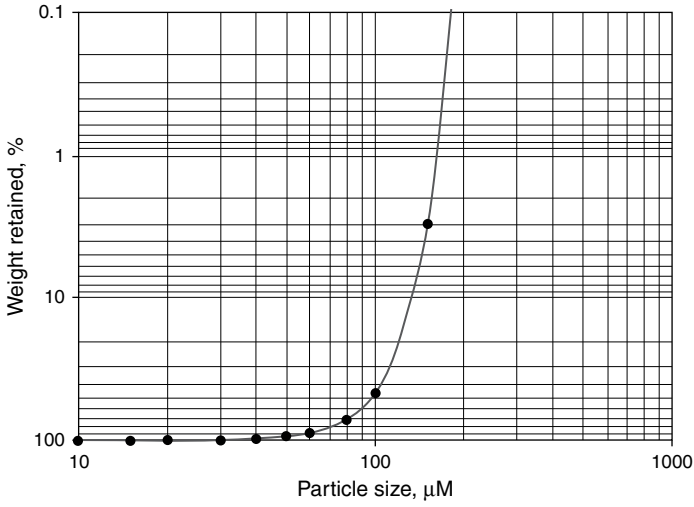


**Figure 6.6** Rosin-Rammler pulverized-fuel size distribution with 3 and 77 percent passing 150 and 75 μm respectively.

## 6.11 Pulverized Fuel Delivery and Firing Systems

Pulverized fuel can be delivered and fired in kilns either directly (direct system) or indirectly (indirect system). The simplest and most commonly used system for pulverized fuel firing is the direct-fired system (Figure 6.7).

The wet coal is fed into a pulverizer along with hot gases drawn from the firing hood. The hot gas temperature is controlled by bleed air. The coal or coke is simultaneously dried and ground in the hot-air swept pulverizer. The pulverizer can be a hammer mill, ring-roll mill, or a ball mill type. The ground particles and air are swept by the primary air fan and delivered to the burner as a dilute suspension of pulverized fuel and air. A combination of solid fuel materials can be fired directly or semi-directly using the system shown in Figure 6.8. Here we envision the firing of coke and coal in a proportion chosen either by design, for economic, or for environmental consideration. Using two pulverizers provides an opportunity to fire either of the fuels independently in the event of a supply shortfall of either fuel. Also, if a moisture-laden coal provides a cheap source of energy, or if one is considering wood or biomass firing as part of an environmental sustainability program, then the second pulverizer can operate as a semi-direct system whereby the alternative fuel can be delivered into a cyclone collector where it can be separated.

It is important to ascertain the appropriate conveying velocities in the pipes that will prevent settling. Low transport velocities or excessively high solids loading may result in unstable operation. If the gas

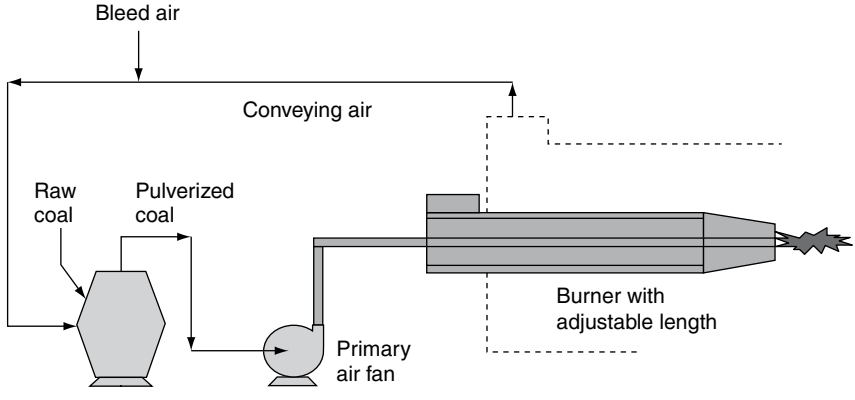


**Figure 6.7** Direct-fired coal combustion delivery system.

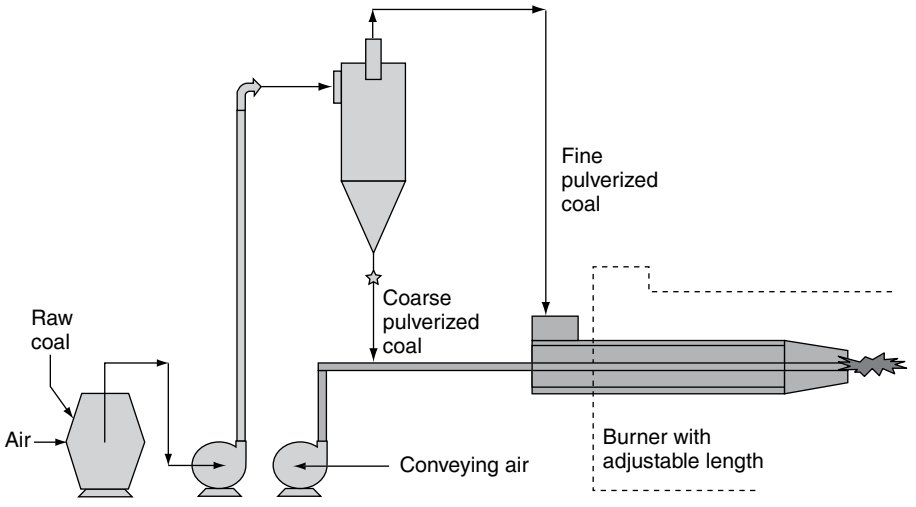


**Figure 6.8** Semi-direct fired coal combustion delivery system.

velocity in a horizontal pipe is reduced progressively, particles will eventually settle along the bottom of the pipe. The minimum velocity at which settling occurs is called the saltation velocity. This is affected by all the resistances to the flow including pipe roughness, pipe diameter, and particle size, but more importantly, by the gas/solid loading. Increased solid loading will violate the gas laws and pressure drop across the pipe may decrease rather than increase with increasing airflow. Minimum transport velocities recommended based on coal milling experience are 15 m/s with a specified minimum air temperature at the mill of 60°C. The minimum figure for air velocity applies to the lowest coal throughput, which is about 30–40 percent of the maximum coal throughput depending upon the turndown ratio. As the coal loading is increased, the airflow should also increase but not proportionately. So therefore, as the coal feed is increased, the transport velocity increases but the air-to-coal ratio decreases. At maximum coal flow, the air-to-coal ratio reaches its minimum, around 1.6:1 wt/wt, and the flow velocity reaches its maximum. Hence by a combination of suitably sized transport pipework and suitably controlled air-to-coal ratios, a system should be operated so that the velocity at minimum throughput is at least 15 m/s and around 25 m/s at maximum throughput (Scott, 1995).

## 6.12 Estimation of Combustion Air Requirement

We have already discussed under practical stoichiometry how the air requirements can be estimated based on the fuel composition (ultimate analysis). The primary and secondary air requirements for combustion of pulverized coal or coke are best estimated by mass and heat balance at the mill. In Appendix 6A we show a calculation taken from Musto (1997) for the primary and secondary air required for coal pulverizer with 4.5 metric ton per hour (10,000 lb/hr) coal feed rate at initial moisture of 15 percent which is required to be ground and dried to 2 percent with a 200 HP mill. In order to estimate the actual primary and secondary air, one has to make some estimation of the evaporation rate, the amount of gas entering the coal mill, and the bleed air required so that the quantity of air that should be vented from the hood off-take can be properly estimated. It shows that for a take-off gas temperature of 315°C (600°F) and vent gas temperature of 76°C (170°F) and allowing ambient air infiltration of 10 percent at 15°C (60°F) the primary air will be about 22 percent of stoichiometric air and 21 percent of total air. The remaining air (about 79 percent) will be the secondary air. With this information we can size a burner using a burner pipe diameter based on a Craya-Curtet parameter of choice bearing in mind the conditions that ensure the desired jet recirculation patterns described in Chapter 3.

## 6.13 Reaction Kinetics of Carbon Particles

In the combustion of pulverized fuel, firing begins with the combustion of volatiles followed by the combustion of the solid particles remaining after pyrolysis, that is, the oxidation of the carbon in the char (carbon and ash). Perhaps the char combustion step is the most important one since it involves heterogeneous reaction of solid and gas and, hence, requires thorough mixing. The burnout of the carbon typically follows a shrinking core model that is depicted in Figure 6.9. In this model a spherical char particle is assumed to be surrounded by a boundary layer of stagnant gas (oxidant and combustion products) several particle diameters thick, through which oxygen diffuses from the free stream and reacts at the surface to form combustion products, which also diffuse outward into the free stream. The generalized equations for transport can be deduced by assuming that in the boundary

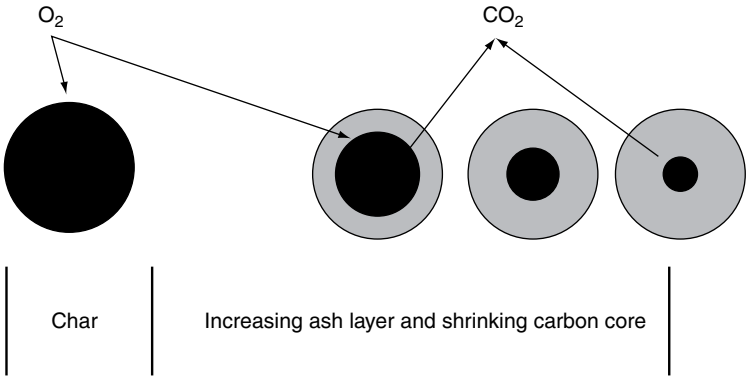


**Figure 6.9** Char burnout model.

layer, oxygen is conserved and that the rate at which oxygen is transported through an imaginary surface at any radius is equal to the rate at which oxygen is transported to the particle surface. The flux of oxygen at the surface of a particle with radius $r$ can be expressed as (Field et al., 1964).

$$rG(r)\frac{R'T_m}{\widetilde{D}M} = p_g - p_s \tag{6.28}$$

where $\widetilde{D}$ is the diffusion coefficient, $R'$ is the gas constant, $M$ is the molecular weight, $T_m$ is the mean temperature, and $p_g$ and $p_s$ represent the oxygen partial pressures in the free stream (subscript g, for gas) and at the surface (subscript s). Equation (6.28) gives the rate of oxygen transport to the particle surface in terms of the concentration of oxygen in the free stream and at the surface.

Since the carbon particle is porous and also char particle in a stagnant environment will leave a residual ash uninterrupted, the diffusion coefficient involves the resistance to flow of oxygen and combustion products through the ash layer and through the porous carbon itself. The rate of reaction of the carbon with oxygen at the reaction front can be expressed in terms of the oxygen partial pressure at the surface and the surface reaction rate constant $k_s$ as

$$q = k_s p_s \tag{6.29}$$

where $q$ is the rate of removal of carbon per unit external geometric surface area, [g/cm$^2$s]. The rate constant $k_s$ may be expressed by the Arrhenius type equation as

$$k_s = A \exp(-E/RT_s) \tag{6.30}$$

where $T_s$ is the surface temperature in degrees Kelvin, and the gas constant $R = 1.986$ cal/mol°K. Typical values of the frequency factor $A$, and the activation energy $E$, for anthracite coal are $A = 8710$ g/cm$^2$ s and $E = 35,700$ cal/mol.

## 6.14 Fuel Oil Firing

Atomization is to liquid fuels as pulverization is to solid fuels. Atomization is required to break down liquid fuel oil into tiny droplets prior to combustion. Droplet combustion follows the same model as char combustion shown in Figure 6.9. The size of the droplets and the way they are dispersed has a critical affect on burner performance. Like pulverized solid fuel, the ignition temperature of fuel oils is much lower than gas, so the mixing is the rate controlling step in the combustion process. Although some light fuel oils, for example kerosene, may readily vaporize and mix with the oxidant prior to ignition, heavy fuel oils, which are frequently used in rotary kilns, need to be spray-atomized into the secondary air to ensure adequate mixing. The droplet combustion process is similar to coal combustion, starting with initial heating and flaming pyrolysis, which releases volatiles and a porous sphere of coke particles known as a *cenosphere*. The volatiles burn at the surface of the droplet as oxygen diffuses to the fuel molecules through the combustion products. Like char, the combustion of the coke follows the shrinking core (see Figure 6.9). Hence, liquid fuels are characterized by their droplet size and burning rate. The burning rate may be used to predict the heat and mass release rates of different-sized droplets as a function of residence time in the kiln environment. Additionally, the time required to completely consume a given size droplet may be easily computed from knowledge of the characteristic burning rate. By performing an energy and mass balance over a single-component, spherical droplet vaporizing in a uniform, quiescent atmosphere (i.e.,

low-Reynolds-number droplet vaporization), the instantaneous rate of droplet evaporation can be expressed by

$$\dot{m}_v = -\frac{\mathrm{d}}{\mathrm{d}t}\left(\frac{\pi}{6}\rho_l d_d^3\right) = -\frac{\pi}{4}\rho_l d_d \frac{\mathrm{d}}{\mathrm{d}t}\left(d_d^2\right) \tag{6.31}$$

and

$$\frac{\mathrm{d}}{\mathrm{d}t}\left(d_d^2\right) = -\frac{8\left(\lambda/c_p\right)}{\rho_l}\cdot\ln\left(1+B_{h,v}\right) \tag{6.32}$$

where $\lambda$ is the thermal conductivity of the gas, and $B_{h,v}$ is a characteristic heat transfer number (Law, 1982) defined as

$$B_{h,v} = \frac{c_p\left(T_a - T_l\right)}{q_v} \tag{6.33}$$

Here $q_v$ is the latent heat of vaporization. The heat transfer number, $B_{h,v}$, represents the ratio of the vaporization potential of the ambient environment to the vaporization energy requirement of the liquid fuel. Integrating Equation (6.32) yields

$$d_d^2 = d_0^2 - K_v \cdot t \tag{6.34}$$

with the evaporation rate constant, $K_v$, defined by Equation (6.32) as

$$K_v = -\frac{8\left(\lambda/c_p\right)}{\rho_l}\cdot\ln\left(1+B_{h,v}\right) \tag{6.35}$$

Equation (6.34) is the so-called "$d^2$ law" which shows that the square of the droplet diameter decreases linearly with time. The equation also reveals that the residence time for complete consumption of a droplet may be expressed as

$$\tau = {d_0^2}/{K_v} \tag{6.36}$$

This demonstrates a quadratic dependence of burnout on the diameter of the initial liquid droplet. For burning droplets, the droplet flame front acts as a nearby source of heat for droplet vaporization, otherwise the mechanism is the same as pure vaporization. For a single-component, uniform droplet burning under quasi-steady gas-phase conditions

$$d_d^2 = d_0^2 - K_c \cdot t \tag{6.37}$$

with the combustion rate constant, $K_c$, defined as

$$K_c = -\frac{8\left(\lambda/c_p\right)}{\rho_l} \cdot \ln\left(1 + B_{h,c}\right) \tag{6.38}$$

and the combustion heat transfer number given by

$$B_{h,c} = \frac{c_p\left(T_\infty - T_l\right) + \left(Y_{O_2,\infty}/\sigma_{O_2}\right)}{q_v} \tag{6.39}$$

where $Y_{O2,\infty}$ and $\sigma_{O2}$ are the oxidizer mass fraction in the far field and the stoichiometric mass fraction of the oxidizer to the fuel, respectively. Therefore, under idealized conditions, the $d^2$ law holds for droplet combustion. However, in reality, what is not accounted for in the $d^2$ law are the effects of multicomponent fuels, transient droplet heating, fuel vapor depletion or accumulation between the droplet and the flame, and various gas-phase transport properties (as functions of concentration and temperature). Experiments have shown that droplet combustion often begins with the droplet heating (transient) period during which the droplet diameter is relatively constant because of thermal expansion offsetting initial weak vaporization. After the transient period, whose duration is dependent on size, ambient environment, and fuel properties, single-component fuels and fuels with narrow volatility ranges typically exhibit $d^2$ law behavior throughout the majority of the droplet burning (Shaddix and Hardesty, 1999). Calculated droplet evaporation and burning rates for diesel No. 2 fuel oil, water, and some pyrolysis oils derived from wood, grasses, and their mixtures are presented in Table 6.4 (Shaddix and Hardesty, 1999). For fuels containing water, such as the pyrolysis liquids derived from biomass, the droplet burning rates are reduced as the water content increases due to the higher heat of vaporization and higher stoichiometric air requirements.

Most atomizers produce a range of droplet sizes with the smallest on the order of a few micrometers in diameter. Large droplets can range anywhere between 100 and 1000 μm (Mullinger et al., 1974). In a typical industrial rotary kiln flame a droplet particle of 100 μm diameter will take about half a second to burn out according to the burning rate calculations presented here. With a residence time of only a few seconds in the freeboard of a rotary kiln, atomization, which produces droplets larger than 200 μm, might not ensure a complete burnout of the fuel. Therefore, in order to ensure carbon burnout and proper flame shape and length in kiln burners, either droplet sizes are made smaller,

**Table 6.4** Calculated Droplet Vaporization and Combustion for Liquid Burnable Fuels (Shaddix and Hardesty, 1999)

| Liquid Fuel | $\rho_l$ (g/ml) | $q_v$ (J/g) | $K_v$ (mm$^2$/s) | $\sigma_{ox}$ | $q_c$ (J/g) | $K_c$ (mm$^2$/s) |
|---|---|---|---|---|---|---|
| Diesel No. 2 | 0.86 | 267 | 0.56 | 12.6 | 41.0 | 0.99 |
| Water | 1.00 | 2257 | 0.099 | – | – | – |
| Biomass derived pyrolysis liquids produced by National Renewable Energy Lab (NREL) | | | | | | |
| NREL 154 (oak) | 1.20 | 613 | 0.25 | 5.6 | 17.6 | 0.52 |
| NREL 175 (poplar) | 1.20 | 711 | 0.23 | 6.3 | 16.0 | 0.45 |
| NREL 157 (switchgrass) | 1.20 | 887 | 0.19 | 8.2 | 19.3 | 0.40 |
| NREL 175 + water | 1.18 | 842 | 0.20 | 5.7 | 14.6 | 0.42 |
| NREL 175 + methanol | 1.16 | 738 | 0.23 | 6.3 | 16.3 | 0.45 |
| NREL 175 + ethanol | 1.16 | 720 | 0.23 | 6.4 | 16.8 | 0.46 |

or larger spray droplets must undergo microexplosions. Microexplosions occur in multicomponent droplets that have a broad range of volatiles as associated with liquid burnable fuels such as solvents or waste-derived liquid fuels. The driving force for microexplosions is the much faster process of thermal transport (diffusion) within the liquids compared to mass transport. The ratio of the thermal diffusivity, $\alpha_l$, and the mass diffusivity, $D_l$, is the dimensionless Lewis number ($Le = \alpha_l/D_l$). Since the droplet surface temperature is at the boiling point of the instantaneous molecular mixture at the surface, it increases rapidly as more volatile components become depleted. The temperature rise at the surface sets up a temperature gradient between the interior and the surface which results in heat transfer to the interior. A microexplosion occurs when the characteristic temperature (superheat limit) is reached by the liquid mixture at any location within the droplet. This limit is about 90 percent of the thermodynamically defined critical temperature at 1 atmosphere pressure (Shaddix and Hardesty, 1999).

## 6.15 Combustion Modeling

As was shown in Figure 6.9, combustion begins with flaming pyrolysis, which is an endothermic reaction requiring initial heat to proceed when the fuel particle, whether liquid droplets or pulverized, reaches a certain threshold temperature. This is followed by the

homogeneous combustion of the released gaseous compounds and the exothermic heterogeneous reaction of the solid carbon particles with the oxygen in the air. Combustion modeling requires knowledge of the kinetics of all the reaction steps involved. However, since the fuel particles are suspended in a surrounding jet fluid in direct-fired systems, the effect of flow on combustion as well as the combustion chamber boundaries are important considerations. We also discussed that mixing is the rate-controlling step in the combustion of pulverized fuels as well as liquid droplets. For a more accurate estimation of the combustion process one must model the turbulent gas-particle flows and combustion simultaneously. In Chapter 3 we presented a set of equations in a reactive flow system involving mass, momentum, and energy conservation (cf., Equations 3.17 through 3.28):

Continuity Equation:

$$\frac{\partial \rho}{\partial t} + \frac{\partial}{\partial x_j}(\rho u_j) = 0$$

Momentum Equation:

$$\frac{\partial}{\partial t}(\rho u_i) + \frac{\partial}{\partial x_j}(\rho u_j u_i) = -\frac{\partial P}{\partial x_i} + \frac{\partial}{\partial x_j}\left[\mu\left(\frac{\partial u_j}{\partial x_i} + \frac{\partial u_i}{\partial x_j}\right)\right] + \rho g_i$$

Concentration Transport Equation:

$$\frac{\partial}{\partial t}(\rho Y_s) + \frac{\partial}{\partial x_j}(\rho u_j Y_s) = \frac{\partial}{\partial x_j}\left(D\rho \frac{\partial Y_s}{\partial x_j}\right) - w_s$$

Enthalpy Transport Equation:

$$\frac{\partial}{\partial t}(\rho c_p T) + \frac{\partial}{\partial x_j}(\rho u_j c_p T) = \frac{\partial}{\partial x_j}\left(\lambda \frac{\partial T}{\partial x_j}\right) + w_s Q_s$$

Arrhenius Equation:

$$w_s = B\rho^2 Y_F Y_{ox} \exp(-E/RT)$$

Equation of State:

$$P = \rho RT \sum Y_s / M_s$$

Ideally, one would numerically model these equations using computational fluid dynamic (CFD) modeling, which we will discuss later.

However, before such tools became available there were qualitative assessments based of the simplification of these equations that helped the burner designer or kiln operator evaluate combustion performance based on a set of rules and experiences. In Chapter 3 we explored, based on the dimensionless numbers derived from the reactive flow conservation equations, the importance of mixing in the combustion process and stated that if the reactants are mixed then the fuel is burnt because mixing is the slowest step. The importance of turbulent mixing in the form of recirculation eddies is that it returns combustion products to the flame front and increases the residence time in the combustion chamber. Although the correct estimation and use of the turbulent kinetic energy (TKE), which is a linear function of retention time, through CFD predictions is preferred, a combination of flow visualization techniques and mixing parameters such as the Craya-Curtet parameter calculations are equally powerful tools that are still used in the industry today. We will explore the two methods to determine the flame character before proceeding to a full CFD analysis.

## 6.16 Flow Visualization Modeling (Acid-Alkali Modeling)

It is said that the technique of modeling of mixing processes using a mixture of dilute acid and alkaline was first employed by Hawthrone in 1939 at MIT in his thesis work on the mixing of gas and air in flames (Moles et al., 1973). He developed a method of accurately modeling physical jet mixing by discharging a jet of dilute sodium hydroxide (NaOH) solution colored with phenolphthalein indicator into a surrounding fluid of dilute hydrochloric acid (HCl), the reaction of which visually simulates the combustion process and thereby the flame boundary. Ruhland (1967) used this technique later to investigate fuel/air mixing and combustion processes in cement kilns. The technique was later employed by Jenkins and Moles (1981) who, with Mullinger, later founded Fuel & Combustion Technology (FCT) to optimize burner operations in rotary kilns. To this date such techniques are still useful and are often employed by kiln burner providers as a viable alternative to CFD modeling. To model the combustion chamber, a physical model of the hood and the combustion zone of the kiln are constructed to an appropriate scale in clear acrylic plastic. In order to simulate combustion, the fuel is represented by the

alkali with the phenolphthalein coloring. Once the alkali is neutralized by the acid, which represents the fuel oxidant (air), the mixture solution becomes clear, thereby providing a visual representation of the physical location where combustion is complete, that is, where all the fuel is presumed consumed. The technique involves isothermal flows. However, in real combustion systems buoyancy effects result due to temperature changes. One way of introducing buoyancy in a cold model such as this is to distort the flows in the physical model so as to make it representative of the full site plant. Hence an essential feature of the technique is to maintain a dynamic similarity. The concentration of the alkali (simulated fuel), and the stoichiometric ratio of the acid (simulated air) and alkali reactions are chosen to represent the correct air-fuel ratio requirement for the particular fuel used in practice. For example, when natural gas is the primary fuel rather than fuel oil, the higher air-fuel ratio requirement for natural gas is represented by higher alkali concentration and the acid flow rate is adjusted to simulate the levels of excess air. Figure 6.10 is an acid-alkali representation of a pulverized fuel flame with a low (Figure 6.10a) and high (Figure 6.10b) burner momentum conditions.

Experience has shown that for a confined flame, sufficient primary air jet momentum is required to create mixing via external recirculation zones. As the acid-alkali model shows, high momentum and, for that matter, intense and perhaps complete mixing, is tantamount to efficient combustion. We discussed in Chapter 4 that, for confined jets, the onset of flame recirculation can be described by the Craya-Curtet

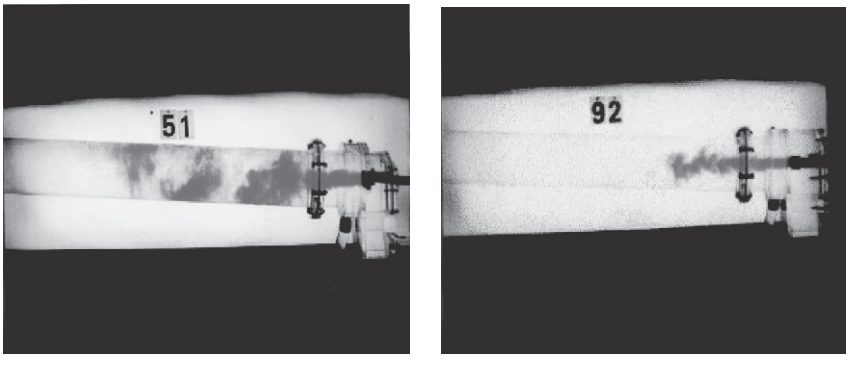


(a) Low burner momentum (b) High burner momentum

**Figure 6.10** Acid-alkali modeling of combustion in rotary kilns; (a) low burner momentum, (b) high burner momentum.

parameter $M$, which is essentially the momentum ratio between the primary and secondary air streams. Although $M$ can be anywhere between zero and infinity ($0 < M < \infty$), practical experience has shown that $M = 1.5$ is the threshold momentum ratio that generates the recirculation associated with good mixing. $M = 1.5$ will ensure that the burner jet will have momentum in excess of that required to entrain all the secondary air in the near field and to cause vortex shedding that returns combustion products to the flame front, resulting in an attached flame (Figure 6.10b). Hence Figure 6.10a representing a low momentum burner has a Craya-Curtet number $M < 1.5$. Experience has also shown that burners with excessively high jet momentum will suffer poor combustion. Some of the adverse effects include inadequate flame length, unstable flame, pulsating flows, and so on. The optimum Craya-Curtet parameter value for coal-fired kilns is somewhere between 1.5 and 2.5. For cement kilns, experience has shown that the short and intensive flames needed to complete the bed reactions are achieved with a Craya-Curtet parameter value between 2 and 2.5. Lime kilns requiring less intense and longer flames operate with $M$ values between 1.5 and 2.0. Employing these techniques provides the kiln engineer or the operator an avenue of evaluating the flame character without resulting to full blown computational fluid dynamics modeling. However, CFD provides a means of achieving all of the above and more including heat fluxes, combustion product, and other species concentrations that are associated with emissions.

## 6.17 Mathematical Modeling Including CFD

Computational fluid dynamics is a virtual prototyping that guides in building accurate flow models by solving transport equations. The features of combustion flows can be analyzed in detail with CFD. In particular, mixing, temperature, flow velocity, flame stability, and concentration of combustion species can accurately be computed for different geometry. CFD modeling of gas flow inside the rotary kiln chamber provides three-dimensional analyses of the general flow pattern by mapping the pressure field and velocity vectors that show recirculation zones, mixing, and resident time within the chamber and further provides temperature and species concentration of the combustion products. It therefore makes it possible to evaluate useful operational parameters of interest for design optimization prior

to prototyping, or troubleshooting an existing design for operational performance.

The physical and chemical phenomena of the reacting flow may be simulated by numerically solving a set of generalized conservation equations for flow (Navier Stokes equations), and an associated set of equations involving enthalpy, combustion, and so on. A fundamental method for the numerical simulation of the governing equations is the finite-difference or finite-element approximations. The formal steps involved in the application of the methods follow four steps (Vichnevetsky, 1981): (i) the domain of the problem is covered by a simple mesh, (ii) values of the numerical solution are labeled at the intersections or nodes of the mesh, (iii) a finite-difference or finite element approximation to the differential equation is formulated in each node resulting in a system of algebraic finite-difference or finite-element equations, and (iv) the system of equations approximating the problem is solved to produce a numerical solution. This process generally involves solving numerically large systems of linear algebraic equations and the corresponding computer algorithms are those of numerical linear algebra. Until recently when computer power improved, it was not possible to apply CFD modeling to industrial rotary kilns because of the large aspect ratio and the large number of mesh points involved to accurately represent the problem. A typical 3 m diameter by 30 m long rotary kiln ($L/D = 10$) may require a couple million mesh points for the calculation domain and require several days or even weeks to execute the program depending on the power of the computer used. However, several CFD providers have improved their modeling capabilities and CFD has become a powerful tool in modeling the complex rotary kiln phenomena including combustion and flames. CFD solves the conservation equations involving mass, momentum, combustion, and enthalpy equations within the boundaries of the kiln. The two-phase flow nature of pulverized fuel combustion requires tracking of the particles as localized sources and brings an added complexity to CFD modeling of such operations. To model the combustion in kilns, mathematical expressions are required for the turbulent reactive flow, coal pyrolysis or devolatilization, homogeneous volatile combustion, heterogeneous char reaction, particle dispersion, radiation, and pollutant emission. There are several CFD providers that offer software packages for the simulation of rotary kiln processes. They all treat the mathematical expressions and the numerical schemes required for their solution slightly differently. We will present some of the generalized equations that are common to combustion modeling.

As pointed out earlier in Chapter 3 and will be covered in more detail later on in this chapter, the flow in a rotary kiln is typically gas-solid turbulent flow with chemical reactions, mainly combustion. The building blocks behind the user-defined functions (UDF) in commercial CFD codes applied to rotary kiln combustion modeling consist of "renormalization group" (RNG) k-ε turbulent model for gas phase and, in the case of pulverized combustion particles, the statistical (stochastic) trajectory model for homogeneous volatile and heterogeneous solid-phase char combustion. The underlying equations are discussed in the next section.

## 6.18 Gas-Phase Conservation Equations Used in CFD Modeling

The set of conservation equations that are solved in most CFD analyses are as presented earlier but expanded to include the stress generation as in Equations (6.40) through (6.45) (Wang et al., 2006).

Continuity:

$$\frac{\partial \rho}{\partial t} + \frac{\partial}{\partial x_i}(\rho u_i) = S_p \tag{6.40}$$

where the variable in the continuity equation represents a source term typical to fuel injection or combustion of particles in a control volume. The components of velocity in a three-dimensional coordinate system are represented by the momentum equation

Momentum:

$$\frac{\partial}{\partial t}(\rho u_i) + \frac{\partial}{\partial x_i}(\rho u_i u_j) = -\frac{\partial p}{\partial x_j} + \frac{\partial \tau_{ij}}{\partial x_j} + \rho g_i + F_i + S_p \tag{6.41}$$

which includes pressure, turbulent shear stresses, gravitational force, that is, buoyancy effects, and the source terms arising from gas-solid interactions. The $\tau_{ij}$ term in Equation (6.41) represents Reynolds stress as

$$-\overline{\rho \tilde{u_i} \tilde{u_j}} = \mu_t \left( \frac{\partial u_i}{\partial x_j} + \frac{\partial u_j}{\partial x_i} \right) - \frac{2}{3}\delta_{ij} \left( \rho k + \mu_t \frac{\partial u_i}{\partial x_i} \right) \tag{6.42}$$

Turbulence modeling is implemented as a closure model for the Reynolds stress with the most commonly used k-ε turbulence model being

k-equation

$$\frac{\partial}{\partial t}(\rho k) + \frac{\partial}{\partial x_i}(\rho k u_i) = \frac{\partial}{\partial x_j}\left[\left(\mu + \frac{\mu_t}{\sigma_k}\right)\frac{\partial k}{\partial x_j}\right] + G - \rho\varepsilon \tag{6.43}$$

ε-equation

$$\frac{\partial}{\partial t}(\rho\varepsilon) + \frac{\partial}{\partial x_i}(\rho\varepsilon u_i) = \frac{\partial}{\partial x_j}\left[\left(\mu + \frac{\mu_t}{\sigma_\varepsilon}\right)\frac{\partial \varepsilon}{\partial x_j}\right] + C_{1\varepsilon}\frac{\varepsilon}{k} - C_{2\varepsilon}\frac{\varepsilon^2}{k} + S_\varepsilon \tag{6.44}$$

where the generation of turbulence denoted by $G$ in Equation (6.43) comprises two terms, (i) the generation of turbulence kinetic energy due to the mean velocity gradients, and (ii) that due to the generation of turbulence kinetic energy due to buoyancy. $S_\varepsilon$ is the turbulence source term in Equation (6.44). The turbulent Navier Stokes equations are presented with the standard nomenclature and the enthusiastic reader is referred to the appropriate CFD literature.

In order to include temperature distribution, the Navier Stokes equations are accompanied by an energy equation that solves for enthalpy ($h = c_p T$). The balance equation for enthalpy is

$$\frac{\partial}{\partial t}(\rho h) + \frac{\partial}{\partial x_i}(\rho u_i h) = \frac{\partial}{\partial x_j}\left(\Gamma_h \frac{\partial h}{\partial x_j}\right) + S_h \tag{6.45}$$

The source term, $S_h$, includes combustion, that is, the heat source and the heat transfer within the system that affect temperature. In rotary kilns, the dominant heat transfer mode is radiation and there are several models to evaluate its value, some of which will be examined in detail later.

CFD providers treat gas-phase combustion by using a mixture fraction model (Wang et al., 2006). The model is based on the solution of the transport equations for the fuel and oxidant mixture fractions as scalars and their variances. The combustion chemistry of the mixture fractions is modeled by using the equilibrium model through the minimization of the Gibbs free energy, which assumes that the chemistry is rapid enough to assure chemical equilibrium at the molecular level. Therefore, individual component concentrations for the species of interest are derived from the predicted mixture fraction distribution.

## 6.19 Particle-Phase Conservation Equations Used in CFD Modeling

Most CFD providers track particles in the reactive flow field by solving the pertinent equations for the trajectory of a statistically significant sample of individual particles that represents a number of the real particles with the same properties. For example, following the Rosin-Rammler size distribution (Figure 6.6), coal particles are tracked using a statistical trajectory model followed by the modeling of the kinetics of devolatilization and subsequent volatile and char combustion as discussed previously in this chapter (Figure 6.9). Models similar to the $d^2$ law presented earlier are used for droplet combustion of atomized fuel oil.

In CFD modeling numerical solutions are sought by discretizing Equations (6.40–6.45) and integrating over each control volume represented by the mesh following

$$\int_V \frac{\partial \rho \phi}{\partial t} \mathrm{d}V + \oint_A \rho \cdot \phi \cdot u \cdot \mathrm{d}A = \oint_A \Gamma \cdot \nabla \phi \cdot \mathrm{d}A + \oint_V S \mathrm{d}V \qquad (6.46)$$

where $\phi$ is the property value, for example, velocity, temperature, species concentration, and so on. Usually, specific to a problem to be analyzed, boundary and initial conditions are provided and these equations are solved iteratively until the convergent criteria are met. A typical mesh generation for the combustion zone of an industrial rotary kiln firing pulverized fuel is shown in Figure 6.11. There is no need to extend the calculation domain to the entire kiln if the focus is to evaluate burner performance.

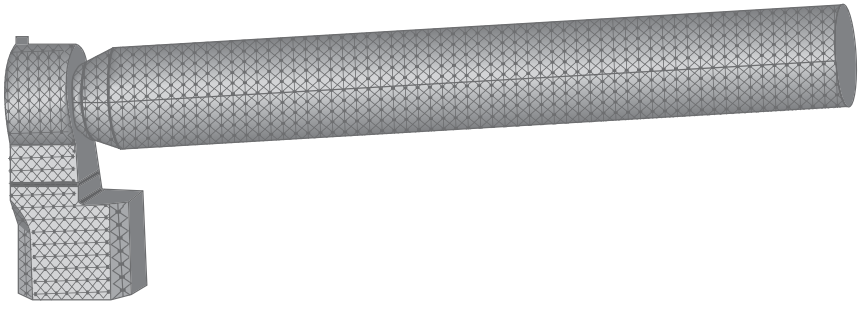

**Figure 6.11** CFD mesh generation for rotary kiln combustion modeling.

## 6.20 Emissions Modeling

### 6.20.1 Modeling of Nitric Oxide (NOx)

Nitric oxide (NOx) is one of the main pollutants in combustion systems and rotary kilns are no exception particularly for pulverized fuel combustion. NOx formation depends on three factors, namely (i) the amount of nitrogen present in the fuel, (ii) the combustion temperature, and (iii) the stoichiometric conditions for the combustion reaction. Hence NOx production is classified into fuel NOx, thermal NOx, and prompt NOx. Some of the mechanisms for the formation of these species during pulverized coal combustion in rotary cement kilns have been described in commercial CFD packages (e.g., FLUENT, CINAR).

#### *6.20.1.1 Fuel NOx*

Most models assume that the fuel-bound nitrogen that is released by the devolatilization of coal is in the form of HCN, or some instantaneous transforms of HCN, which in turn form the base species of NO formation. It is believed that the HCN not only contributes to fuel NOx formation but also to some destruction of NOx and that the net formation might depend on the chemical as well as the thermal state of the mixture. The global chemical reactions involved for coal flames might therefore be expressed as

$$\mathrm{HCN} + \mathrm{O_2} = \mathrm{NO} + \mathrm{Products} \tag{6.47}$$

$$\mathrm{HCN} + \mathrm{NO} = \mathrm{Products} \tag{6.48}$$

Kinetic studies have shown that the principal pathways of NO formation and reduction by hydrocarbon radicals are

$$\mathrm{NO} + \mathrm{CH_2} \leftrightarrow \mathrm{HCN} + \mathrm{OH} \tag{6.49}$$

$$\mathrm{NO} + \mathrm{CH} \leftrightarrow \mathrm{HCN} + \mathrm{O} \tag{6.50}$$

$$\mathrm{NO} + \mathrm{C} \leftrightarrow \mathrm{CN} + \mathrm{O} \tag{6.51}$$

where the reactions proceed mainly in the forward path. Detailed kinetic studies have also established the following set of reactions (Visser, 1991)

$$\mathrm{CH_4} + \mathrm{H} = \mathrm{CH_3} + \mathrm{H_2} \tag{6.52}$$

$$\mathrm{CH_3} + \mathrm{OH} = \mathrm{CH_2} + \mathrm{H_2O} \tag{6.53}$$

$$CH_2 + H = CH + H_2 \tag{6.54}$$

$$CH + H = C + H_2 \tag{6.55}$$

which, for hydrocarbon diffusion, the flames can be considered, within reasonable accuracy, to be in partial equilibrium.

The concentration of H radicals in the post flame regions of hydrocarbon diffusion flames have been observed to be on the same order as the $H_2$ concentration, and the OH radical can be estimated by the observed partial equilibrium of the reaction

$$OH + H_2 = H + H_2O \tag{6.56}$$

in these flames.

These fast chemistry multi-mixture fraction combustion models and similar models have been incorporated into several CFD packages including CINAR, FLUENT, and others.

#### *6.20.1.2 Thermal NO*

One source of thermal NO is the oxidation of the molecular nitrogen in the combustion air. The activation energy, the threshold energy required for the formation of thermal NO is high, hence its formation is highly temperature dependent and important only at high temperatures. Thermal NO is usually modeled by the so-called "extended Zeldovich" mechanism (Westenberg, 1971), which follows these reaction mechanisms:

$$O + N_2 \leftrightarrow NO + N \tag{6.57}$$

$$N + O_2 \leftrightarrow NO + O \tag{6.58}$$

$$N + OH \leftrightarrow NO + H \tag{6.59}$$

Reactions (6.57) and (6.58) are important and reaction (6.59) is significant only under highly fuel rich conditions. The reaction step (6.59) is usually neglected for coal combustion because coal flames are normally very lean in fuel.

#### *6.20.1.3 Prompt NO*

Prompt NO is formed by the attack of hydrocarbon fragments on molecular nitrogen in the flame zone. The contribution of prompt NO to the total NO is normally very small in rotary kilns and is usually ignored.

### 6.20.2 Modeling of Carbon Monoxide (CO)

The predictions of CO are based on a thermodynamic equilibrium computer program in which the chemical equilibrium compositions for assigned thermodynamic states are calculated. Most often temperature and pressure, calculated from the main CFD code, are used to specify the thermodynamic state. The method for evaluating the equilibrium compositions is based on the minimization of Gibbs energy as mentioned earlier (Wang et al., 2006).

## 6.21 CFD Evaluation of a Rotary Kiln Pulverized Fuel Burner

The combustion of pulverized coal in a 3.66 m (12 ft) rotary kiln was modeled using the commercial CFD code offered by FLUENT, which employs a user-defined function (UDF) that one can program and that can be dynamically loaded with the software's solver. The problem at hand involves a burner hood arrangement with a primary air jet issuing from a burner pipe and secondary air from a product cooler at the bottom and discharged into the combustion chamber. The objective function is to compare the performance of two burner nozzles with two different flow areas, one with a swirl vane (Burner A), and the other with a 7.62 cm insert installed for flame stabilization (Burner B; Figure 6.12). The kiln geometry and operating conditions including pulverized fuel flow rate and tip velocities are presented in Table 6.5. The flow was such that the Craya-Curtet parameters were respectively 1.34 and 1.82 for Burner A and Burner B.

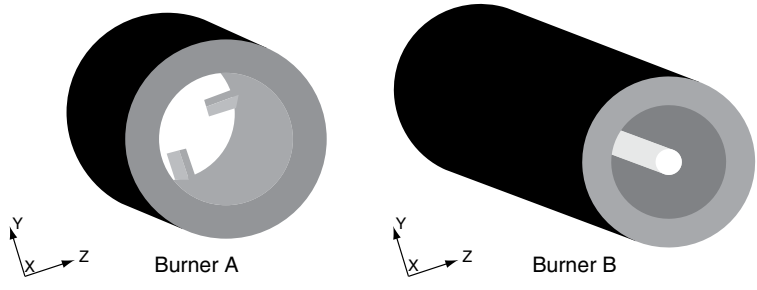


**Figure 6.12** Burner nozzle geometry for pulverized fuel combustion in a rotary kiln. Left: swirl vanes; Right: center insert for flame stabilization.

**Table 6.5** Input Variables for CFD Modeling of a Rotary Kiln Combustion System

| | Burner A | Burner B |
|---|---|---|
| Kiln diameter (m) | 3.66 | 3.66 |
| Stoichiometric air/fuel ratio(wt/wt) | 8.41 | 8.41 |
| Fuel flow rate (kg/s) | 2.38 | 2.47 |
| Primary air (% of stoichiometric) | 22.75 | 23.02 |
| Secondary air temperature (°C) | 760.0 | 760.0 |
| Primary air temperature (°C) | 63.89 | 73.89 |
| Excess air (%) | 4.50 | 4.50 |
| Fuel specific gravity | 1.30 | 1.30 |
| Nozzle diameter (mm) | 336.55 | 298.18 |
| Burner insert diameter (mm) | None | 76.2 |
| Burner pipe flow area ($m^2$) | 0.0889 | 0.0844 |
| Primary air flow rate (kg/s) | 4.55 | 4.78 |
| Primary air nozzle velocity (m/s) | 62.21 | 83.75 |
| Secondary air velocity (m/s) | 5.44 | 5.62 |
| Momentum ratio | 0.10 | 0.11 |
| Craya-Curtet parameter | 1.34 | 1.82 |

The burner performance, as predicted by the CFD results, is presented in Figures 6.13 through 6.16. The model is validated when predicting the interaction of the jet flow from the nozzle and secondary air from the cooler. Figure 6.13 shows slightly asymmetrical flow with the nozzle of Burner A without an insert and an almost symmetrical flow Burner B, which has the flame stabilizer. It has been shown that for self-similar turbulent eddies the vortex rotation period must be a linear function of the diffusion timescale. The effect of flame stabilizers includes increased tip velocity due to lesser flow area and manifests as a higher momentum ratio between the primary and secondary air, thereby inducing stronger recirculation zones as depicted by the vortex shedding. The turbulent kinetic energy (TKE) is a linear function of time. For confined flows, where recirculation eddies return solid particles to the flame front, stronger TKE means longer retention for particles at the flame front for combustion. For a good mixing, one would expect increased diffusion exhibited by internal and external recirculation zones with return of solid particles to the flame region. Hence, Burner B, with the flame stabilizer, provides a better mixing as expected due to a high Craya-Curtet parameter. The Craya-Curtet number for Burner B was 1.82 compared to 1.34 for Burner A. As we have

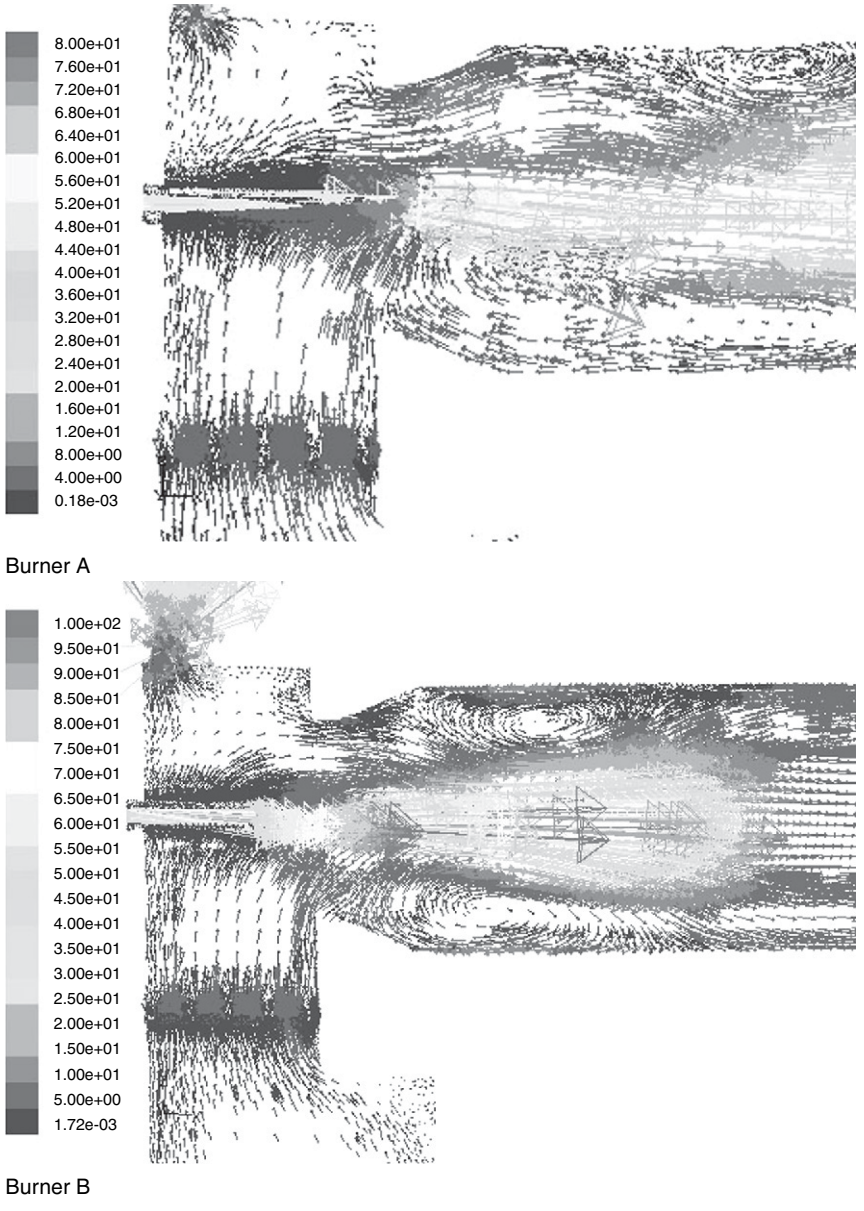


**Figure 6.13** CFD results for the velocity distribution of the flow field in the combustion zone of a rotary kiln with a pulverized fuel burner showing interaction between primary air jet and the entrained secondary air.

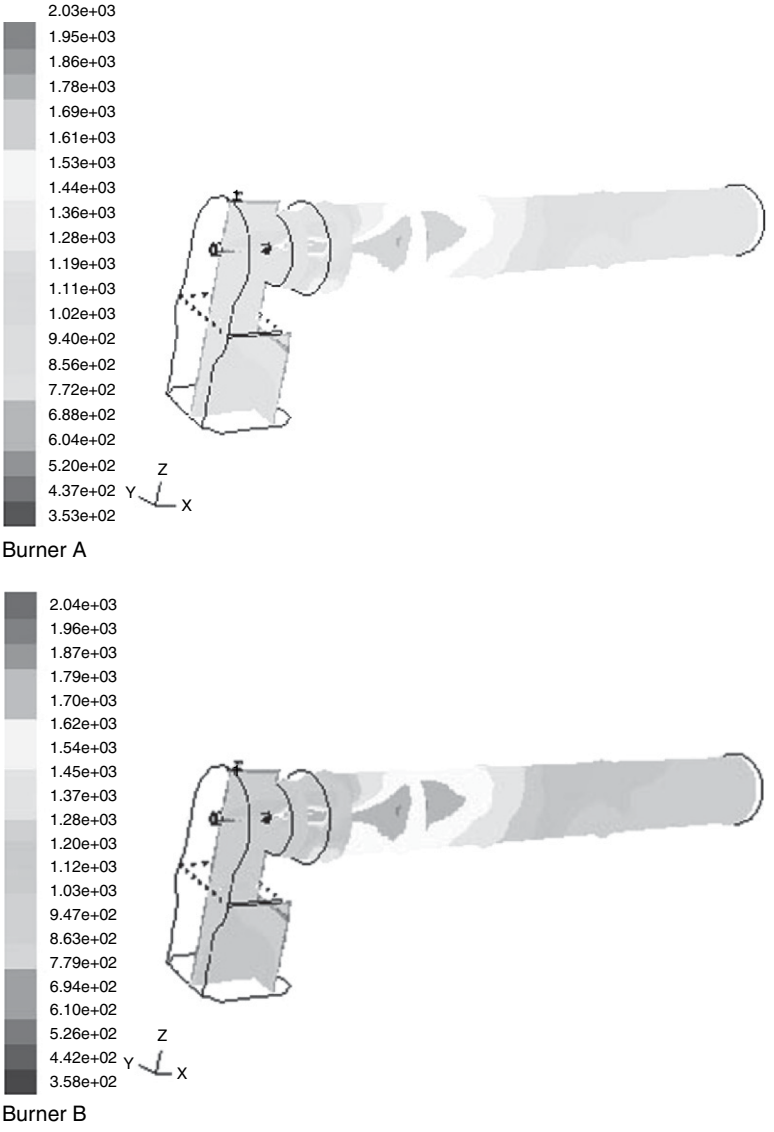


**Figure 6.14** CFD predictions for three-dimensional temperature distribution mapping the combustion and flame shape.

already discussed, a nozzle with a higher Craya-Curtet parameter is expected to provide a more intense flame and this flame will be drawn closer to the burner tip as the CFD results show (Figures 6.14 and 6.15). As indicated in the theoretical section, combustion efficiency depends on the ratio of the diffusion time to that of the chemical

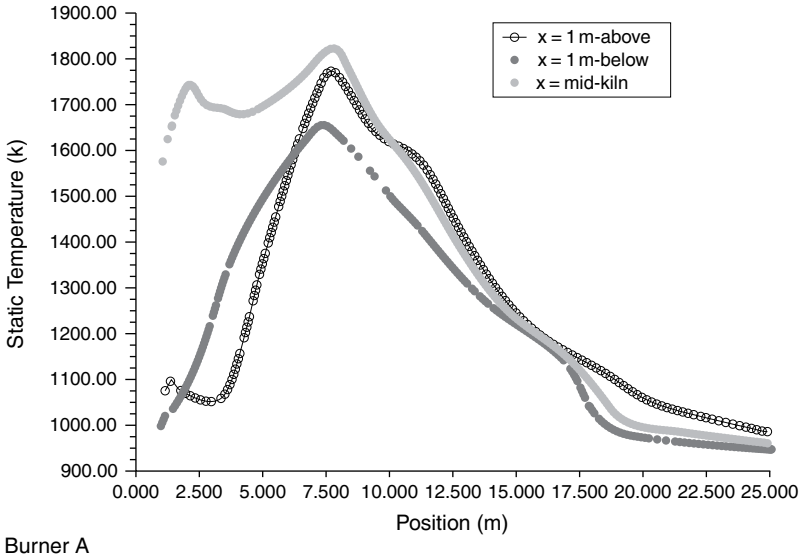


Burner A

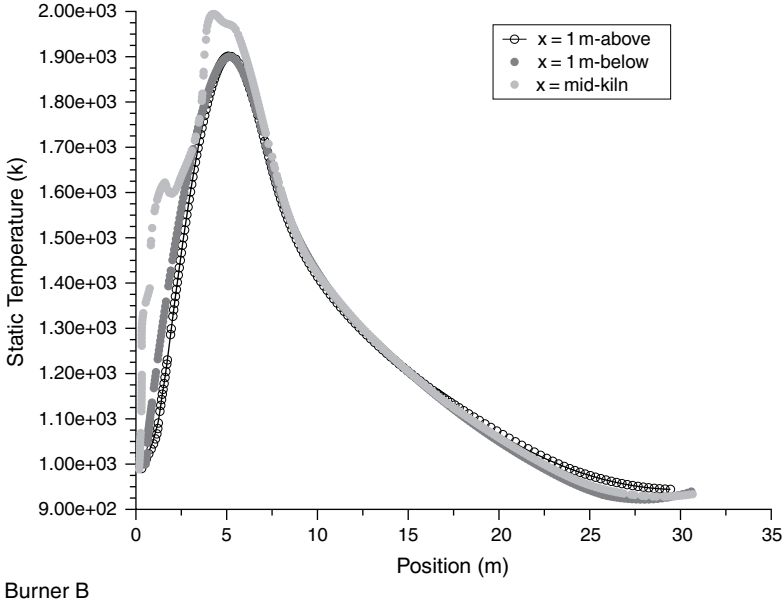


Burner B

**Figure 6.15** CFD predicted axial temperature profiles.

reaction. Since diffusion has the lowest timescale, it determines the combustion outcome. The bad news is that due to the intensity of the flame associated with the flame stabilizer, a three-fold increase in the NOx emission is predicted based on the equations shown earlier. As a result of the more intense recirculation eddies (vortex shedding) a higher rate of combustion products including unburned char particles return to the flame front for a prolonged residence time. The burnout of coal particles for Burner B completes at almost half of the axial distance of burnout in Burner A (Figure 6.16).

It has been demonstrated that CFD has the capacity to predict the flame character and the temperature profiles observed by experience. Although intrinsic details of the combustion and flame

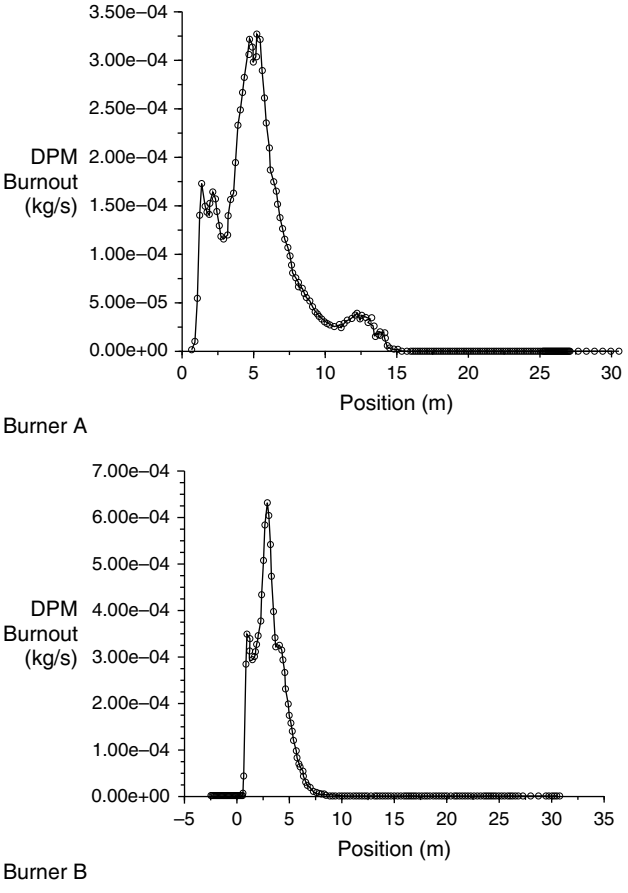


**Figure 6.16** Predicted coal particle burnout.

can be obtained from such models, large computational demands are required as shown by the large number of calculation cells in Figure 6.12. Even with a high-speed computer, it is not uncommon to expect 3–4 days of real time running before results are obtained for a medium sized rotary kiln. The good news is that qualitative results by flow visualization and partially quantitative estimates (e.g., the use of similarity parameters such as that of Craya-Curtet) can suffice with some experience in making interim judgments on rotary kiln combustion performance.

## References

M. A. Field, D. W. Gill, B. B. Morgan, and P. G. W. Hawksley. *Combustion of Pulverized Coal*. British Coal Utilization Research Association (BCURA), Leatherhead, UK, 1967.

B. G. Jenkins and F. D. Moles. "Modelling of heat transfer from a large enclosed flame in a rotary kiln," *Trans. IChemE*, 59, 17–25, 1981.

C. K. Law. "Recent advances in droplet vaporization and combustion," *J. Prog. Energy Combust. Sci.*, 8, 171–201, 1982.

F. D. Moles, D. Watson, and P. B. Lain. "The aerodynamics of the rotary cement kiln," *J. Inst. of Fuel*, December, 353–362, 1973.

P. J. Mullinger and N. A. Chigier. "The design and performance of internal mixing multijet twin fluid atomizers," *J. Inst. Fuel*, 47, 251–261, 1974.

R. L. Musto. "Coal firing of cement kilns," presented at Cement Manufacturing Technology Seminar, Pennsylvania State University, 1978.

S. L. Polak. Alcan report #A-RR-1475-71-08, Arvida, Canada, 1991.

W. Ruhland. "Investigation of flames in the cement rotary kiln," *J. Inst. Fuel*, 40, 69–75, 1967.

D. Scott. *Coal Pulverizers—Performance and Safety*. IEA Coal Research, 1995.

C. R. Shaddix and D. R. Hardesty. "Combustion properties of biomass flash pyrolysis oils." Final project report, Sandia National Laboratories Report SAND99-8238, 1999.

R. Vichnevetsky. *Computer Methods for Partial Differential Equations*. Prentice Hall, Englewood Cliffs, NJ, 1981.

B. M. Visser. *Mathematical Modeling of Swirling Pulverized Coal Flames*. PhD Dissertation, IFRF, 1991.

K. C. Watson. *Energy Conversion*. West Publishing Co., New York, 1992.

S. Wang, J. Lu, W. Li, J. Li, and Z. Hu. "Modeling of pulverized coal combustion in cement rotary kiln," *Energy & Fuels*, 20, 2350–2356, 2006.

A. A. Westenberg. "Kinetics of NO and CO in lean, premixed hydrocarbon-air flames (Reaction kinetics of NO and CO formation in lean premixed hydrocarbon-air flames)," *Combustion Sci. and Technol.*, 4, 59–64, 1971.

# Appendix 6A

## Calculation of Primary Requirements for 10,000 lb/hr Coal Combustion

CALCULATIONS FOR ESTIMATING COMBUSTION AIR USING COAL/COKE PULVERIZER

| | | SI | | | SI |
|---|---|---|---|---|---|
| Feed rate [FR]: | 10000 lb/hr | 4535.9 kg/hr | Specific heat capacity of gas, cp | 0.24 Btu/lb. °F | 1004.9 J/kg K |
| Initial moisture content [IM]: | 15% | 15% | Specific heat capacity of solid, cp | 0.3 Btu/lb. °F | 1256.1 J/kg K |
| Final moisture content [FM]: | 2% | 2% | Latent Heat of Evap. | 996.3 Btu/lb | 553.5 cal/g |
| Initial gas temperature [IT]: | 600 F | 315.6 C | Specific volume of dry air @ 170°F | 15.88 $ft^3$/lb | |
| Vent gas temperature [VT]: | 170 F | 76.7 C | Specific volume of water vapor @ 170°F | 25.3 $ft^3$/lb | |
| Product temperature [PT] | 130 F | 54.4 C | Infiltration [INFIL]: | 10% | 10% |
| Mill horsepower [BHP] | 100 | 981 kW | Ambient temperature [AT]: | 60°F | 15.6°C |
| | | | Entering gas, E | lb/hr | |

EVAPORATION CALCULATION

| | | |
|---|---|---|
| Evaporation = FR x [(IM-FM)/(1-FM)] | 1326.5306 lb/hr | 601.7 kg/hr |
| Product Rate [PR] = [FR - EVAP]. | 8673.469 lb/hr | 3934.2 kg/hr |
| Dry Solids Rate [DSR] = [PR x (1-FM)] | 8500 lb/hr | 3855.5 kg/hr |
| Moisture remaining in coal = [PR - DSR] | 173.469 lb/hr | 78.7 kg/hr |

GROSS HEAT INPUT FROM GAS

| | | |
|---|---|---|
| GROSS-HEAT = E x Cp X (IT - AT) | 1993325 Btu/hr | 584.0 kW |

VENT QUANTITY

PRIMARY AIR + EVAPORATION

| | | |
|---|---|---|
| **PRIMARY AIR:** Entering gas (E) + infiltration (10% of E) | 16918.7 lb/hr | 7674.2 kg/hr |
| TOTAL VENT QUANTITY | 18245.18 lb/hr | 8275.9 kg/hr |

CALCULATION OF ENTERING GAS [E]

System heat input:

Contribution from mill motor
BHP × 0.75 × 2545 — 190875 Btu/hr — 55.9 kW

Net heat input from gas [E]
E × Cp × ΔT = ΔH × E
ΔH — 103.2
Net heat input from gas = 103.2E

Total heat input =
A1 103.2E + 190875 Btu/hr

Heat absorbed and lost:

B1 Heat absorbed in evaporation:
EVAP x [Cp(VT-AT) + Latent Heat of evap.] — 1467540.8 Btu/hr — 430.0 kW

C1 Heat absorbed in heating the product:
PR × Cp × ΔT
Solids: 178500
Moisture: 12142.857
Total 190642.86 Btu/hr — 55.9 kW

D1 Radiation heat loss:
5% of E = 0.05 × 103.2E = 5.16E — 5.16

E1 Infiltration heat loss:
10% of E = 0.1E × Cpg × ΔT = 2.64E — 2.64

Estimate E by balance as:
Heat Input = Heat absorbed and lost
A1 + B1 = C1 + D1 + E1
103.2E + 190,875 = 1,467,541 + 190642 + 5.16E + 2.64E
E = 15380.6 Btu/hr — 4.5 kW

VENT VOLUME (AT TEMP)

| | | |
|---|---|---|
| Primary (Dry Air) | 268668.22 $ft^3$/hr | |
| Water Vapor | 33561.224 $ft^3$/hr | |
| Total | 302229.44 $ft^3$/hr | |
| Primary Air | 5037.1574 ACFM | |
| STOICHIOMETRIC AIR/FUEL RATIO (SAR) | 9 wt/wt | 9 wt/wt |
| Theoretical air requirement = SAR × DSR | 76500 lb/hr | 34699.9 kg/hr |
| For the kiln to operate at 5% excess air | 5% | |
| Actual air = | 80325 lb/hr | 36434.9 kg/hr |

**SECONDARY AIR**

| | | |
|---|---|---|
| SA = ACTUAL AIR - PA | 63406.347 lb/hr | 28760.7 kg/hr |
| Primary air percent (of total air) | 21.1% | |
| Primary air percent (of stoic. air) | 22.1% | |